Chapter 21A. Summary of the Mineral Information Package for the Khanneshin Carbonatite Area of Interest

Contribution by Robert D. Tucker, Harvey E. Belkin, Klaus J. Schulz, Stephen G. Peters, and Kim P. Buttleman

Abstract

The Khanneshin carbonatite is a deeply dissected igneous complex of Quaternary age that rises approximately 700 meters above the flat-lying Neogene sediments of the Registan Desert, Helmand Province, Afghanistan. The complex consists almost exclusively of carbonate-rich intrusive and extrusive igneous rocks, crudely circular in outline, with only three small hypabyssal plugs of leucite phonolite and leucitite outcropping in the southeastern part of the complex. The complex is broadly divisible into a central intrusive vent (or massif), approximately 4 kilometers in diameter, consisting of coarse-grained sövite and brecciated and agglomeratic barite-ankerite alvikite; a thin marginal zone (less than 1 kilometer wide) of outwardly dipping (5°–45°). Neogene sedimentary strata; and a peripheral apron of volcanic and volcaniclastic strata extending another 3–5 kilometers away from the central intrusive massif. Small satellitic intrusions of biotite-calcite carbonatite, no larger than 400 meters in diameter, crop out on the southern and southeastern margin of the central intrusive massif.

In the 1970s several teams of Soviet geologists identified prospective areas of interest for uranium, phosphorus, and light rare earth element (LREE) mineralization in four regions of the carbonatite complex. High uranium concentrations are reported in two regions; the greatest concentrations are confined to silicified shear zones in sandy clay approximately 1.1 kilometers southwest of the peripheral part of the central vent. An area of phosphorus enrichment, primarily occurring in apatite, is present in coarse-grained agglomeratic alvikite, with abundant fenite xenoliths, approximately 750 meters south of the periphery of the central vent. Lastly, an area of prospective LREE mineralization was identified within extensively veined and dike-intruded ankerite-barite alvikite in the outer portion of the central vent near its contact with Neogene sedimentary rocks.

Three reconnaissance missions to the Khanneshin carbonatite were completed by scientists of the U.S. Geological Survey. Two of these were to the area of light rare earth element (LREE) enrichment, which is the primary subject of this summary.

Two types of REE mineralization occur. Type 1 REE mineralization consists of semiconcordant, symmetrically banded veins and discontinuous seams, up to 0.5 to 0.7 meters thick and several tens of meters long. These occur throughout a vertical thickness of 150 meters in ankerite-barite alvikite of the LREE area. The symmetrically banded veins and seams are defined by yellow-weathering zones, symmetric around a dark central zone, that are enriched in khanneshite-(Ce), barite, strontianite, and secondary REE minerals (synchysite-(Ce) and parisite-(Ce)). The dark central zone, consisting primarily of ankeritic dolomite, barite, apatite, and strontianite, also has trace khanneshite-(Ce). These symmetric banded veins and seams alternate with dark, meter-thick layers of ankerite-barite alvikite that is the wall rock. In some veins the REE carbonate minerals form dense crystal aggregates, presumably crystallizing from immiscible droplets, which comprise up to 30 percent by volume of the vein. Type 1 mineralized rocks average 19.9 weight percent Ba, 3.61 weight percent Sr, and 2.78 weight percent total LREE ($\sum$ LREE = sum of La, Ce, Pr, Nd). The values of $\sum$ LREE for eight average whole-rock analyses range between 6.23 and 1.83 weight percent.

Type 2 REE mineralization occurs in discordant dikes and tabular sheets, up to tens of meters thick and hundreds of meters long, which are filled with primary igneous minerals that crystallized directly from magma or a late-stage hydrothermal fluid. These REE-enriched igneous rocks are of two types: those enriched in fluorine and those enriched in phosphorus. The igneous rocks enriched in

fluorine have as their REE-bearing minerals idiomorphic phenocrysts of khanneshite, together with synchysite-(Ce), bastnäsite-(Ce), and calkinsite-(Ce) of likely secondary origin. The igneous rocks enriched in phosphorus have as their REE-bearing minerals idiomorphic phenocrysts of carbocernaite-(Ce), together with parisite-(Ce) of secondary origin. The Type 2 mineralized rocks average 11.1 weight percent Ba, 5.36 weight percent Sr, and 3.28 weight percent ∑ LREE (sum of La, Ce, Pr, Nd). The values of ∑ LREE for 14 average whole-rocks range between 5.98 and 0.49 weight percent.

A magmatic origin is indicated for the Type 2 discordant dikes and tabular sheets. Based on textural and field evidence, the semiconcordant veins and discontinuous seams (Type 1 mineralization) may have formed in the presence of REE-rich hydrothermal fluids. It is possible that both types of REE mineralization may be penecontemporaneous, having formed in the marginal zone of a carbonate-rich magma, highly charged with volatile constituents, carbon dioxide, fluorine, and phosphorus, and strongly enriched in barium, strontium, and the LREE.

Both types of REE-enriched rocks are comparable in grade to the world-class Bayan Obo (China) and Mountain Pass (California, USA) deposits, which are also greatly enriched in the LREE. Based on several assumptions, and employing a simple geometry for the mass, we estimate that at least 1 million metric tons of LREE may be present in the Khanneshin Carbonatite Area of Interest. . This comports well with the probabilistic estimate of 1.4 Mt (million metric tons of undiscovered REE resources in all of south Afghanistan (Peters and others, 2007). In addition to the LREE, the Khanneshin carbonatite is greatly enriched in barium (>10 weight percent), strontium (>6 weight percent), phosphorus (~2 weight percent), and uranium (>0.05 weight percent). A resource calculation of these elements was not attempted.

21A.1 Introduction

China's dominance as the producer of more than 95 percent of world output of rare earth elements (REE), its decision to restrict exports of rare earth product, and the rapid increase in worldwide consumption of rare earth products have heightened concern about the future availability of REE. As a result, countries such as the United States, Japan, and member nations of the European Union face a future of limited supplies and high prices for rare earth products unless other sources are found.

Carbonatites are intrusive alkaline igneous rocks composed of more than 50 volume percent calcite or other carbonate minerals. They are a highly prospective source for the REE (model 10, Singer, 1986 a,b).

In southern Afghanistan, the primary area of interest is centered within the Khanneshin carbonatite complex with its U-Th, P, and REE mineral occurrences (Abdullah and others, 1977). Based on the aeromagnetic data from Sweeney and others (2006), a larger permissive tract was delineated to include the north- to northwest-striking carbonatite dikes to the east and west of the Khanneshin, which follow the shape of the aeromagnetic anomalies beneath sand and gravel of the Sistan Basin (fig. 21A-1; Sweeney and others, 2006). A favorable tract, cb01, was identified by Peters and others (2007) to include the carbonatite dikes and central volcanic zone of the Khanneshin as well as the area outlined by the aeromagnetic anomaly.

21A.2 Previous Work

The Khanneshin carbonatite is the primary area of interest for three prospective non-fuel resources: REE, uranium, ,and phosphorus . The prospective resources were first identified and delineated by Soviet geologists (Abdullah and others, 1975; Yeremenko, 1975; Cheremitsyn and Yeremenko, 1976; Alkhazov and others, 1978). Rare earth element mineralization occurs mostly within the northeast marginal zone of the central intrusive stock. High uranium concentrations have been reported in many rocks throughout the carbonatite complex, but the greatest concentrations are confined to silicified shear zones in sandy clay approximately 750 meters (m) southwest of the peripheral part of the central vent. A secondary zone of uranium mineralization is located in the northern marginal zone of the central massif. Finally, phosphorus is present in significant amounts, principally as apatite in

rudaceous agglomerate, fenite xenoliths, and alvikite. Other commodities that may be present in significant, but as yet undiscovered, amounts include barite, fluorite, nepheline, niobium, tantalum, zirconium, and copper. In addition to the Khanneshin carbonatite, alkali syenite intrusive igneous rocks, consisting of volcanoes and intrusive plugs and dikes, occur throughout south Afghanistan (Abdullah and others, 1975; Vikhter and others, 1976, 1978). Based on the regional geology, and Monte Carlo calculations, Peters and others (2007) estimated a 50-percent probability of one or more undiscovered deposits of REE and niobium in south Afghanistan. The mean estimated tonnage of these undiscovered resources is 1.4 Mt (million metric tons) REEand 3.5 Mt Nb, respectively (Peters and others, 2007).

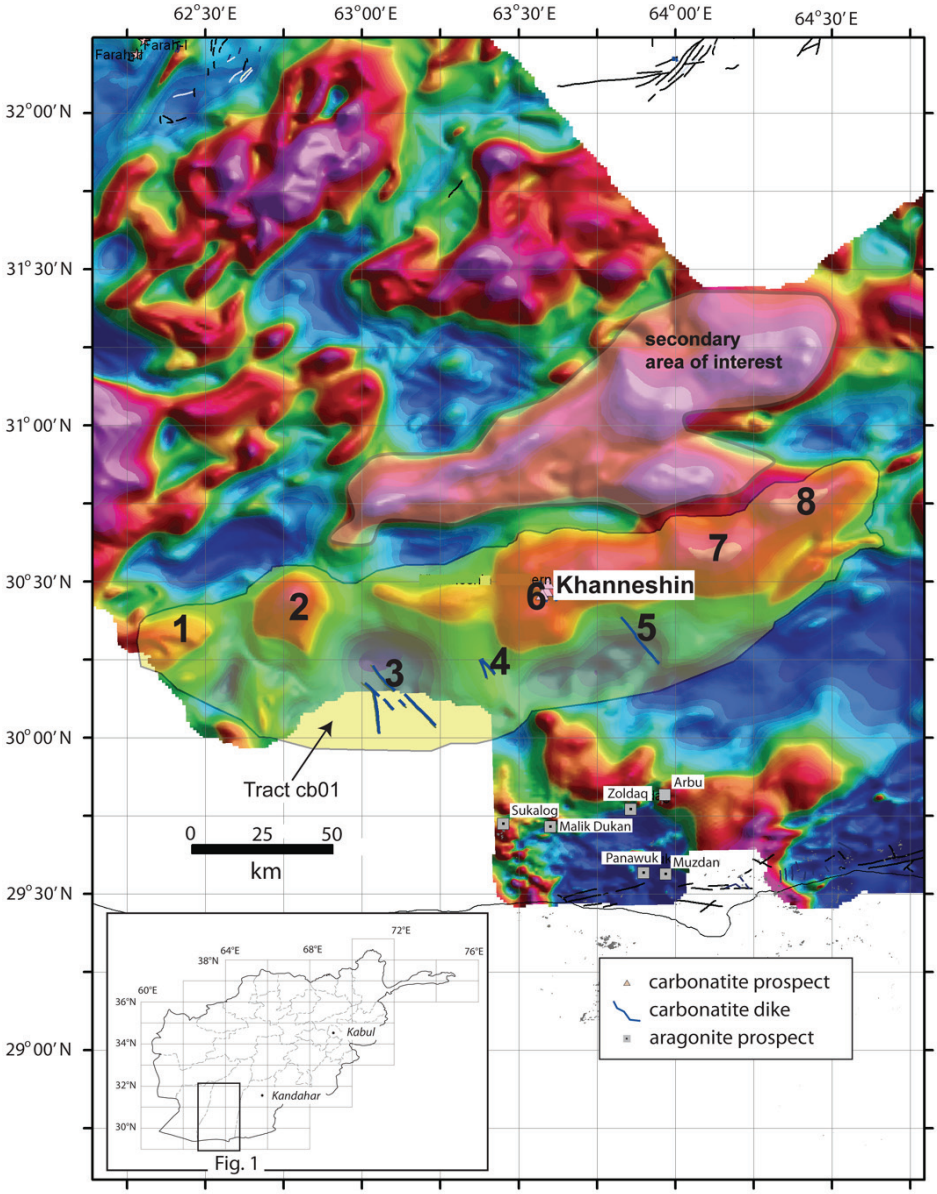

Figure 20A–1. Aeromagnetic map (Sweeney and others, 2006) showing permissive tract of U-P-REE mineralization (cb01) in the Helmand Basin in southern Afghanistan. Numbers one thru eight refer to possible alkaline igneous centers within the tract. These targets formed the basis for the probabilistic estimate of U, P, Nb, and REE resources in Peters and others (2007). The Khanneshin complex is the only exposed carbonatite in south Afghanistan. Additionally, to the north, an aeromagnetic anomaly was designated by the U.S. Geological Survey-Afghanistan Geological Survey Assessment Team as a secondary area of interest for undiscovered REE resources (Peters and others, 2007).

21A.3 Metallogeny

Common economic deposits in carbonatite (model 10, Singer, 1986a) are apatite-magnetite and REE deposits in zoned igneous complexes. The zonation is defined by a central plug of carbonatite or syenite breccia surrounded by ring dikes and cone sheets of carbonatite-related rock types (Hogarth, 1986; Woolley, 1989). Apatite-magnetite and REE-enriched rocks tend to occur in iron- and magnesium-rich carbonatites bearing abundant dolomite, ankerite, and siderite. Associated rocks with these include pyroxenite, feldspathic pyroxenite, picrite porphyrites, dunite, ijolite, nepheline syenite and their volcanic equivalents. Alkalic fenitized wall rocks may also be common. Igneous textures are typically hypidiomorphic-granular and poikiloblastic, but breccia may also be abundant, particularly where magma of the central vent is highly charged with volatile constituents.

Carbonatites range in age from Archean to Holocene. Typically they exhibit a complex history of igneous crystallization with several episodes of injection and eruption of multiple magma types. These magmas are commonly enriched in alkali- and alkali-earth elements, but other elements, such as uranium, thorium, barium, strontium and the rare earth elements, may be present in high concentrations as well. Owing to the high enrichments of incompatible elements and volatile constituents, late deuteric and metasomatic alteration commonly accompanies their emplacement and crystallization. Carbonatites are typically emplaced into continental shields undergoing regional extension, and they are usually related spatially to regional-scale faults and lineaments such as the East African rift system.

Accessory ore minerals in common carbonatite may include pyrrhotite, ilmenite, molybdenite, chalcopyrite, pyrite, pyrochlore, sphalerite, galena, anatase, and brookite. Rarely, such as in the Palabora carbonatite, copper and gold are reported. In carbonatites enriched in phosphorus and iron, important ore minerals are apatite, magnetite, pyrochlore, columbite, and perovskite. In contrast, carbonatites highly enriched in the REE also have high concentrations in barium, strontium, and iron or magnesium. In these rocks, common accessory minerals include barite, strontianite, siderite, rhodochrosite, ankerite, bastnaesite, parisite, monazite, and breunnerite. In many carbonatites, the economic ore minerals are typically disseminated and banded.

The alteration of wall rock and xenoliths associated with carbonatites is accompanied by growth of alkali feldspar, aegerine, alkali hornblende, chlorite, and sphene. This fenitization, or alkali metasomatism, is a result of the passage of alkali-rich fluids through the wall rock during magma emplacement. The ores associated with carbonatites are commonly restricted to carbonatite dikes, sills, breccias, sheets, and veins, but they may also be present in satellitic intrusions associated with the complex. Deep chemical weathering may also form goethite- and clay-rich soils highly enriched in phosphate, niobium, and REE. Geophysical signatures typically consist of radiometric anomalies, magnetic anomalies, and high gravity anomalies. Geochemical signatures are elevated concentrations of Ba, Ce, Cu, Eu, La, Mn, Mo, Nb, P, Pb, S, Sm, U, V, Th, Ti, Y, Zn, and Zr; high concentrations of B, Be, Hf, Li, Sn, Ta, and W are rare. According to Singer (1986b) carbonatite complexes may contain economic grades of U,Th, Ti, Fe, Cu, vermiculite, Zr, or P, and these commodities may be in different parts of the complex than the Nb-rich parts. Mean tonnage for most deposits is 60 million metric tons, and most deposits contain between 16 and 220 million metric tons. Mean niobium grade (weight percent Nb2O5) is 0.58, and mean rare earth oxide grade (weight percent RE_2O_5) is 0.35 (Singer, 1986b).

In Afghanistan, carbonatite and alkali syenite intrusive igneous rocks are present as small volcanic plugs, minor intrusive stocks, and dikes in the Helmand Basin (fig. 21A–1). The largest and most important igneous center is the Khanneshin carbonatite, situated 5 kilometers (km) south of the Helmand River.

21A.4 Geology

The Khanneshin carbonatite, first described by Yeremenko (1975), occurs within the Early Quaternary volcanic rocks south of the Helmand River. The igneous complex is broadly divisible into four parts (figs. 21A–2, 21A–3): a central vent, approximately 4 km in diameter; a thin marginal zone (< 1 km wide) of outwardly dipping (5-40°) Neogene sedimentary strata that comprise the basement to

the igneous complex (fig. 21A–4*a*); a peripheral apron of volcanic and volcaniclastic strata extending another 3–5 km away from the central vent; and small satellitic intrusions of subvolcanic origin, no larger than 400 m in diameter, that crop out on the southern and southeastern periphery of the central intrusive massif.

The following petrogenetic history is taken from Cheremitsyn and Yeremenko (1976) with modification by Vikhter and others (1978).

The Khanneshin complex consists of igneous rocks of several generations. The initial phase was explosive eruption of ankerite alvikite from the central vent. This was followed by forceful emplacement of coarse-grained sövite in the same vent. The presence of strongly metasomatized "glimmerites" and fenites within and around the central vent (fig. 21A–4*c*) suggests extensive fluorine, sulfate, and phosphate enrichment at depth, concurrent with extensive fracturing and emplacement of carbonatite radial dikes (fig. 21A–4*d*). This phase ended with emplacement of REE-enriched ankerite-barite carbonatite in the northeast margin of the central vent (fig. 21A–2).

The succeeding phases commenced as explosive eruption of common alvikite of the satellitic extrusive stocks and vents. These include various agglomerates, lava flows, and tuffs, including fine-grained carbonatites. The final phase of activity was the eruption and emplacement of critically undersaturated silicate magma. These are represented by the flows of leucite phonolite and brecciated plugs of leucitite in the southeastern part of the complex (figs. 21A–2, 21A–3).

The rocks of the Khanneshin complex are assigned an early Quaternary age because they intrude fossiliferous sedimentary rocks of Neogene age, and they are overlain by unconsolidated deposits of Middle-Upper Quaternary age. An unpublished K-Ar age of 610,000 years, cited as personal communication by Whitney (2006), supports this contention.

21A.4.1 Rocks of the Central Vent

The bulk of the igneous massif is made up of rocks of the central vent. They consist of medium- and coarse-grained carbonatite (sövite) confined to a central stock approximately 2-3 km in diameter. Also present is fine- to medium-grained ankerite-barite carbonatite (alvikite) agglomerate that forms a nearly continuous ring, 0.8-1.5 km wide, surrounding the central stock of sövite. At the margin of the central vent, where the intrusive rocks are in contact with Neogene sedimentary rocks, the Neogene strata are strongly altered, brecciated, and invaded by dikes that form an outwardly dipping sequence of discolored and metasomatized albite- and calcite-rich fenites (figs. 21A–4*a,c,d*).

21A.4.2 Rocks of the Volcanic Apron

Pyroclastic and volcaniclastic sedimentary rocks of the Khanneshin area are variegated and banded in their structural and textural features. They form an extensive apron, thickest in the northeast and southeast part of complex, and nearly absent in the west and northwest part of the complex (fig. 21A–4*e*). At least three major eruptive sequences are recognized, some of them linked to intrusive rocks of the central vent (Alkazov and others, 1978), but in general the chemistry and petrography of the volcanic rocks is not well known. In a broad sense, the volcanic formations of the Khanneshin complex are similar to many of the world's carbonatite associations, both in mineralogy and chemistry. An interesting feature of the Khanneshin complex, however, is the overwhelming abundance of carbonatite and the paucity of silicate-rich igneous rocks. Based on discordant field relations with the volcanic apron, the few plugs of leucitite that are present at Khanneshin were emplaced very late in the petrogenetic cycle during the last phase of igneous activity.

The lowest part of the volcanic sequence, near the central vent, consists of dark-red coarse- to medium-grained poorly indurated volcanigenic tuff and sandstone. Within these are abundant thick layers of ferruginous carbonate and carbonate-rich ash. The higher parts of the volcanic sequence are, in general, composed of bright orange-red rocks characterized by a noticeably lower degree of iron enrichment of carbonate, on the whole, by finer grain size. The highly sorted nature of these rocks, and abundant cross-bedding, suggests a significant amount of sedimentary reworking.

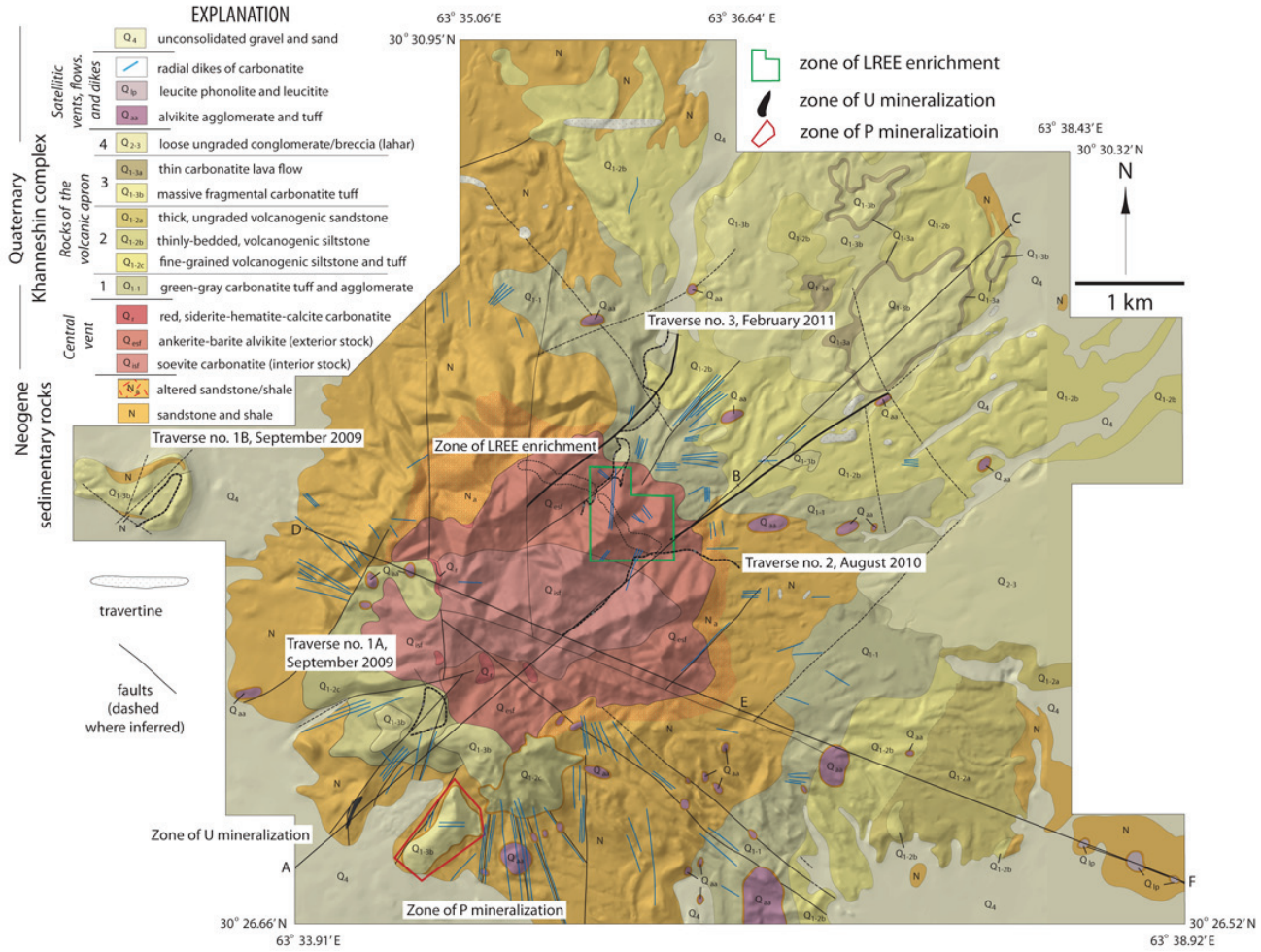

Figure 21A–2. Geologic map of the Khanneshin carbonatite, after Cheremitsyn and Yeremenko (1976), showing the principal bedrock divisions of the complex: (1) The central intrusive vent (or massif), composed of sövite and medium- to fine-grained alvikite agglomerate. The LREE prospect is located in the northeast portion of the central intrusive vent. (2) Neogene sedimentary strata, partly metasomatized, upturned away from the central intrusive vent. (3) The apron of volcanic and volcano-sedimentary strata. (4) Small satellitic intrusive rocks and volcanic plugs, mostly on the southern peripheral margin of the complex, which includes alvikite, sövite, and leucite phonolite. Cross-sectional lines shown in figure 21A-3.

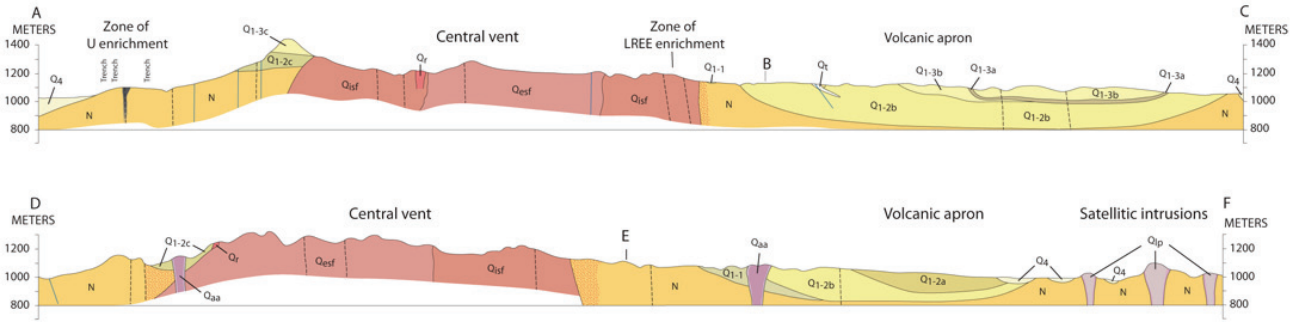

Figure 21A–3. Two lines of cross section (fig. 21A-2) through the Khanneshin carbonatite. Line A-B-C: A northeast-southwest line of section through the REE-enriched area and the zone of uranium mineralization. Line D-E-F : A northwest-southeast line of section through the central intrusive vent and plugs of leucite phonolite.

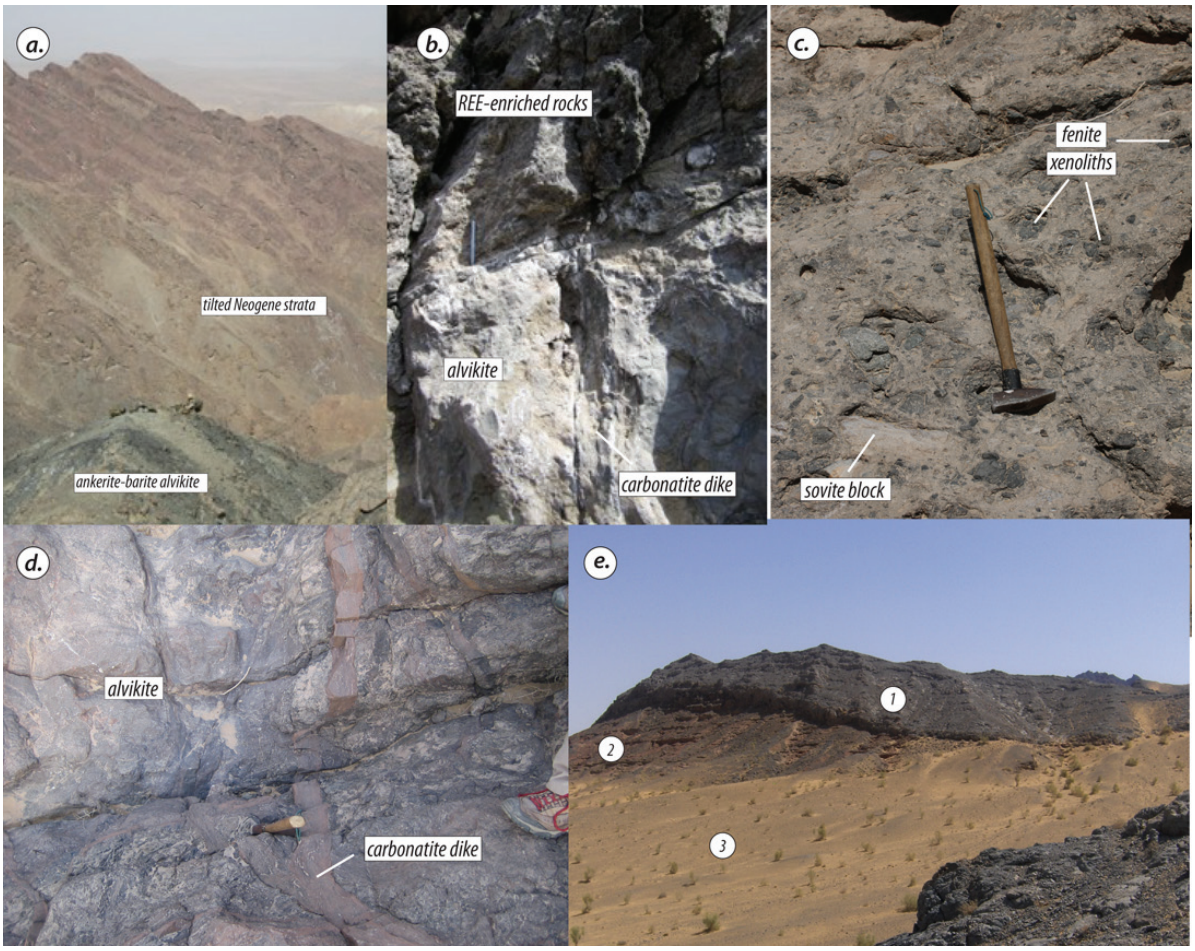

Figure 21A–4. Field photographs of the key rock types and their relations within the central intrusive vent and volcanic apron. (*a*) View to the northwest from the zone of LREE enrichment showing the Neogene strata (background) dipping modestly north and away from the intrusive rocks of the central vent (foreground). Note the rugged relief and person for scale. (*b*) Unconformable relation between alvikite of the REE-enriched rocks (above) and normal carbonatite-intruded alvikite (below) of the marginal zone, central intrusive vent. Pen for scale. (*c*) Common agglomeratic alvikite of the central vent. Here, in the eastern margin of the central vent, the marginal fine-grained alvikite rocks contain abundant xenoliths of fenitized country rock ("glimmerite") and sövite. Hammer for scale. (*d*) Common alvikite of the central vent, here with few xenoliths, intruded by fine-grained dikes of carbonatite (alvikite). Compare with (*c*), above. (*e*) View of the volcanic rocks of the southwest apron (1) showing their relation to older Neogene strata (2) and younger Recent gravels (3). Photographs by Robert D. Tucker, U.S. Geological Survey.

Coarse-grained breccia is present in volcanic agglomerate immediately north of the central vent. These deposits contain blocks of sövite and ankerite-barite carbonatites, several centimeters to several meters in diameter, cemented with green-brown carbonate. In some localities, the blocks of sövite and alvikite are weakly banded, indicating a very crude stratification within the breccia. The presence of fragmental ankerite-barite alvikite suggests that the breccia is a tuffaceous product of the intrusion, perhaps linked to explosive eruption of the REE-enriched alvikites described below.

The southeastern part of the volcanic apron consists of orange-red tuffs that are overlain by massive green tuffs and tuffaceous sediments with pronounced lenticular laminations. The latter rocks are poorly cemented, crystal-lithic tuffs with fragments of ankerite sövite (30–70 volume percent), calcite (5–10 volume percent), phlogopite (2–8 volume percent), and apatite (2–3 volume percent).

21A.4.3 Satellitic Vents, Dikes, and Minor Intrusive Rocks

Six large plugs and several small intrusive masses of coarse-grained carbonatite crop out in the south, southeast, and west part of the complex (figs. 21A–2, 21A–3). These are heterogeneous in composition and texture but, in general, banded and spotted biotite-calcite sövites dominate. The largest of the intrusive plugs contains coarse- and very coarse-grained xenoliths of sövite, biotite-rich "glimmerites" (mica-rich inclusions), and potassium feldspar-rich country rock (fenites). In rare instances, very large (>1 m diameter) inclusions of coarse-grained sövite and "glimmerite" are very abundant, and outcrops have the appearance of giant intrusive breccias.

Three small plugs of leucitite and leucite phonolite crop out in the southeast part of the volcanic apron. These are the only bodies of silicate rock in the Khanneshin complex. The leucite phonolites are dense, massive green-gray rocks with a thinly banded, finely spotted structure and porphyritic texture. Locally they exhibit a spheroidal parting. The phenocrysts (50–70%) consist of idiomorphic leucite crystals measuring 0.2–0.5 millimeters (mm) in diameter. The groundmass consists of sanidine, fine acicular aggregates of aegerine, and minute crystals of nepheline, leucite, and carbonate.

21A.5 Prospects and Anomalies

Carbonatites are of economic interest because they may contain major and unique deposits of several commodities including iron, phosphorus, the rare earth elements, barium, strontium, niobium, uranium, thorium, fluorine, and lead. Studies by Soviet geologists in the 1970s showed that the Khanneshin complex is enriched in high levels of barium and strontium and thus highly favorable for hosting major deposits of phosphorus, uranium, and the rare earth elements. The Soviet teams identified three such prospective areas of phosphorus, uranium, and REE enrichment (fig. 21A–2).

21A.5.1 Uranium Prospect in the Southwest

The uranium contents of the Khanneshin igneous rocks are quite high, typically ranging between 50 to 100 parts per million (ppm). Two zones of uranium mineralization were first identified by Soviet field teams in 1975 (Cheremitsyn and Yeremenko, 1976). The largest zone, most enriched in uranium, is situated 700 to 800 m southwest of the central vent within tuffaceous sandstone of Neogene age. There, uranium mineralization occurs as a north-northeast-trending zone of intense brecciation approximately 200 m wide and 500 m long. Within this zone, the tuffaceous sandstones are intensively brecciated with thin veins of aragonite and chalcedony. Individual lode veins, up to 8 m wide and 100 m long, are impregnated with bright-yellow autuntite ($Ca(UO_2)_2(PO_4)_2 \cdot$ 10-12 H_2O). Whole-rock analyses of the load veins yield assays of 8.04 to 9.63 weight percent uranium, and 0.0036 to 0.0003 weight percent thorium.

21A.5.2 Uranium Prospect in the North

The second zone of uranium mineralization is located 2 to 3 km north of the central vent, also within Neogene sandstone near the periphery of the cone. This zone, too small to be shown in figure 25A–2, is also characterized by extensive silicification (chalcedony); the largest vein is a 1- to 1.5-m--thick zone approximately 100 m long. In this zone, uranium assays of 0.1 weight percent and 0.5 weight percent were determined. Verification of these data by X-ray fluorescence analysis indicates actinide concentrations between 0.0058 and 0.0152 weight percent uranium and 0.0018 and 0.0115 weight percent thorium.

21A.5.3 Phosphorus Prospect in the South

Apatite is the principal phosphorus-bearing mineral in rocks of the Khanneshin complex. It is common in most intrusive igneous rocks, and especially in agglomeratic alvikite with abundant xenoliths of metasomatized country rocks (that is, fenite). Apatite is concentrated in the broken and disaggregated xenoliths, commonly with the assemblage magnetite-apatite-forsterite ± aegerine-acmite, and also as a matrix mineral in agglomerate. Apparently fenitization was a metasomatic process that

involved the complexing and transportation of phosphorus, iron, and REE. According to Cheremitsyn and Yeremenko (1976), the apatite in these rocks is a rare-earth fluoro-apatite (britholite family). The xenoliths assay 8.3 weight percent P_2O_5 and contain 1.0 to 1.5 weight percent LREE (mostly Ce). The rudaceous agglomerate assays 1.55 to 2.29 weight percent P_2O_5.

Eight zones of apatite enrichment were delineated by the Soviet field teams; all are in alvikite agglomerate on the southern flank of the central vent. The principal area of phosphorus enrichment is indicated in figure 21A–2.

Soviet scientists also assayed alluvial gravel and sand in intermittent streams of the northern and eastern part of the central vent. The assays averaged approximately 1 weight percent P_2O_5, and thus placer phosphorus prospects are unlikely to be present.

21A.5.4 The LREE Prospect

A high content of REE is characteristic of the sövitic rocks, as well as the barium- and strontium-rich ankerite-barite alvikites. In the 1970s, Soviet geologists identified a polygonal area having extreme LREE enrichment in the northeast margin of the central vent (Q_{isf}; fig. 21A–2). Two traverses were completed by USGS scientists across the northern and southern corners of the zone of REE enrichment. The traverses are indicated in figure 21A–2. The traverse of August 2010 just touched the southern edge of the REE zone of mineralization, and the traverse of February 2011 crossed the northern corner of the REE mineralization zone. In the course of this work, extremely unusual rocks and minerals were observed, some of them highly enriched in strontium, barium, and LREE (table 21A–1), and more than 50 rock samples, representing the principal rocks of the mineralized zone, were collected for geochemical analysis and scanning electron microscopy. The result of our field and analytical work is summarized below and reported in Tucker and others (2011).

21A.5.4.1 REE Mineralization

Two styles of REE mineralization occur.

Type 1.—Concordant, symmetrically banded veins and seams (fig. 21A–5). Type 1 REE mineralization consists of concordant, symmetrically banded, veins and discontinuous seams, up to 0.5 to 0.7 m thick and several tens of meters long. The layers of REE enrichment consist of two outer bands of yellow-weathering minerals symmetrically disposed about a dark central band. The bands of yellow-weathering minerals consist of khanneshite-(Ce), barite, strontianite and secondary synchysite-(Ce), and parisite-(Ce). The central, dark-colored band consists primarily of ankeritic dolomite, barite, apatite, and strontianite, as well as trace khanneshite-(Ce). These symmetric bands of highly mineralized rock are layered with weakly mineralized ankerite-barite alvikite (that is, the host wall rock) for more than 150 m of exposed vertical section.

Texturally, there is abundant evidence that the REE carbonates formed late in the petrogenetic history, possibly from immiscible fluid droplets (fig. 21A–6). Backscattered electron images demonstrate that khanneshite-(Ce), the primary REE mineral, forms spheroidal mineral aggregates or late fibrous overgrowths on interstitial dolomite and calcite. The average diameter of the spheroidal aggregates, interpreted as REE-rich droplets of immiscible liquid, is 100 micrometers. In still other instances, REE-rich bands of barite, strontianite, and khanneshite-(Ce) appear to have crystallized from a fluid which was introduced into brecciated dolomitic ankerite of the host alvikite. In all examples, the REE minerals crystallized late in the mineral petrogenesis. In some veins the REE carbonate minerals form dense crystal aggregates comprising 50 percent (by volume) of the vein.

Type II.—Discordant tabular sheets (fig. 21A–7). Type 2 REE mineralization occurs in discordant dikes and tabular sheets, up to tens of meters thick and hundreds of meters long, which are filled with primary igneous minerals that crystallized directly from magma or a late-stage hydrothermal fluid. These REE-enriched igneous rocks are of two types; those enriched in fluorine, and those enriched in phosphorus. The igneous rocks enriched in fluorine have as their REE-bearing minerals idiomorphic

phenocrysts of khanneshite-(Ce), together with synchysite-(Ce), bastnäsite-(Ce), and calkinsite-(Ce) of likely secondary (alteration) origin. The igneous rocks enriched in phosphorus have as their REE-bearing minerals idiomorphic phenocrysts of carbocernaite-(Ce), together with parisite-(Ce) of secondary origin.

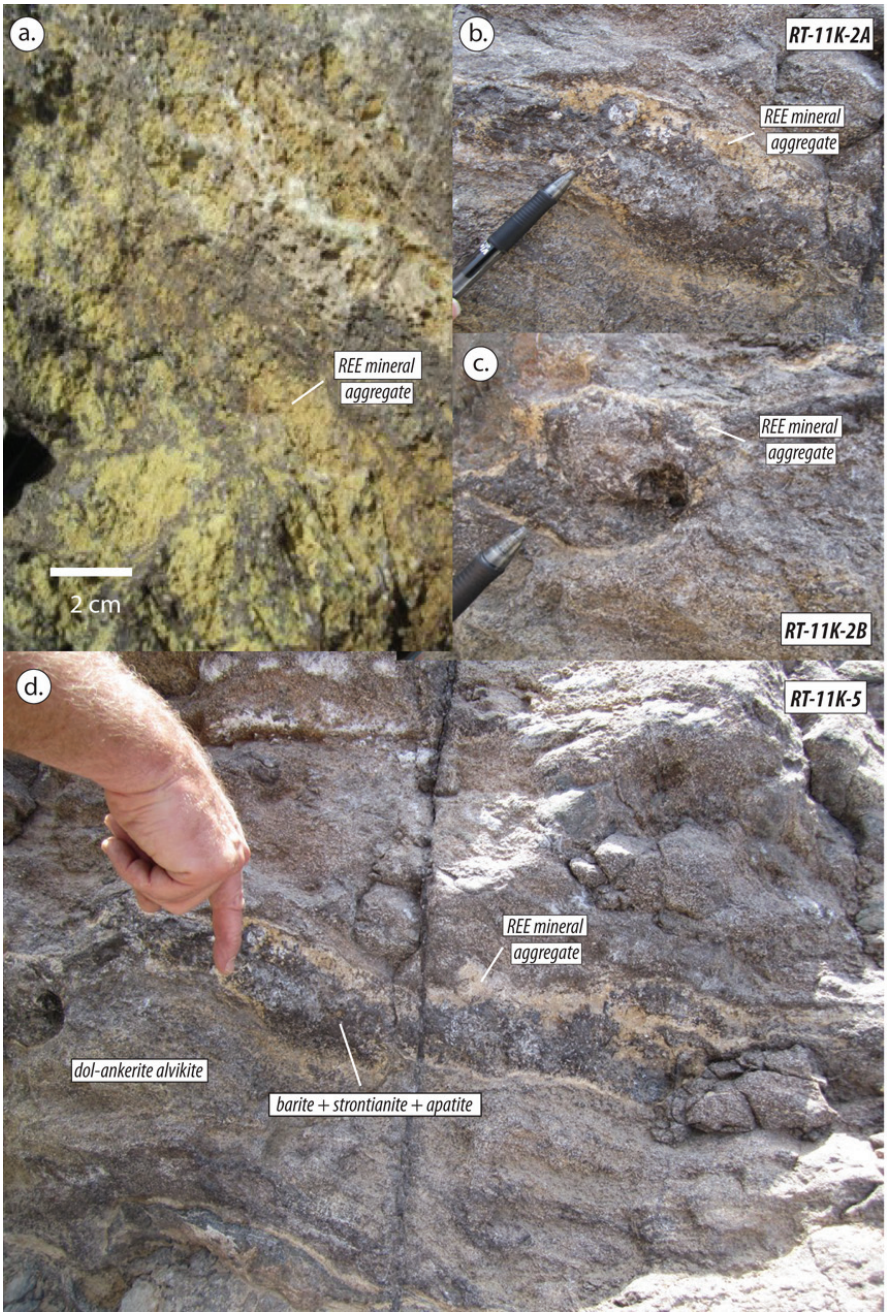

Figure 21A–5. Examples of concordant REE mineralization (Type 1) in the marginal zone of the central intrusive vent, February 2011 traverse (fig. 21A-2). (*a*) Photograph of common alvikite in the REE-enriched zone showing the pitted nature and abundant yellow-weathering indicating the presence of REE carbonate minerals. (*b*) Photograph of the concordant symmetric bands of mineralized alvikite at outcrop RT-11K-2, February 2011 traverse. (*c*) Photograph of a partially rotated concordantly mineralized band implying high fluidity of the mineralized rocks. Outcrop near RT-11K-3, February 2011 traverse. (*d*) Photograph of alvikite showing the mineralized bands at station RT-11K-5. The concordant bands of mineralized alvikite alternate with common dolomite-ankerite alvikite at the scale of centimeters. Photographs by Robert D. Tucker, U.S. Geological Survey.

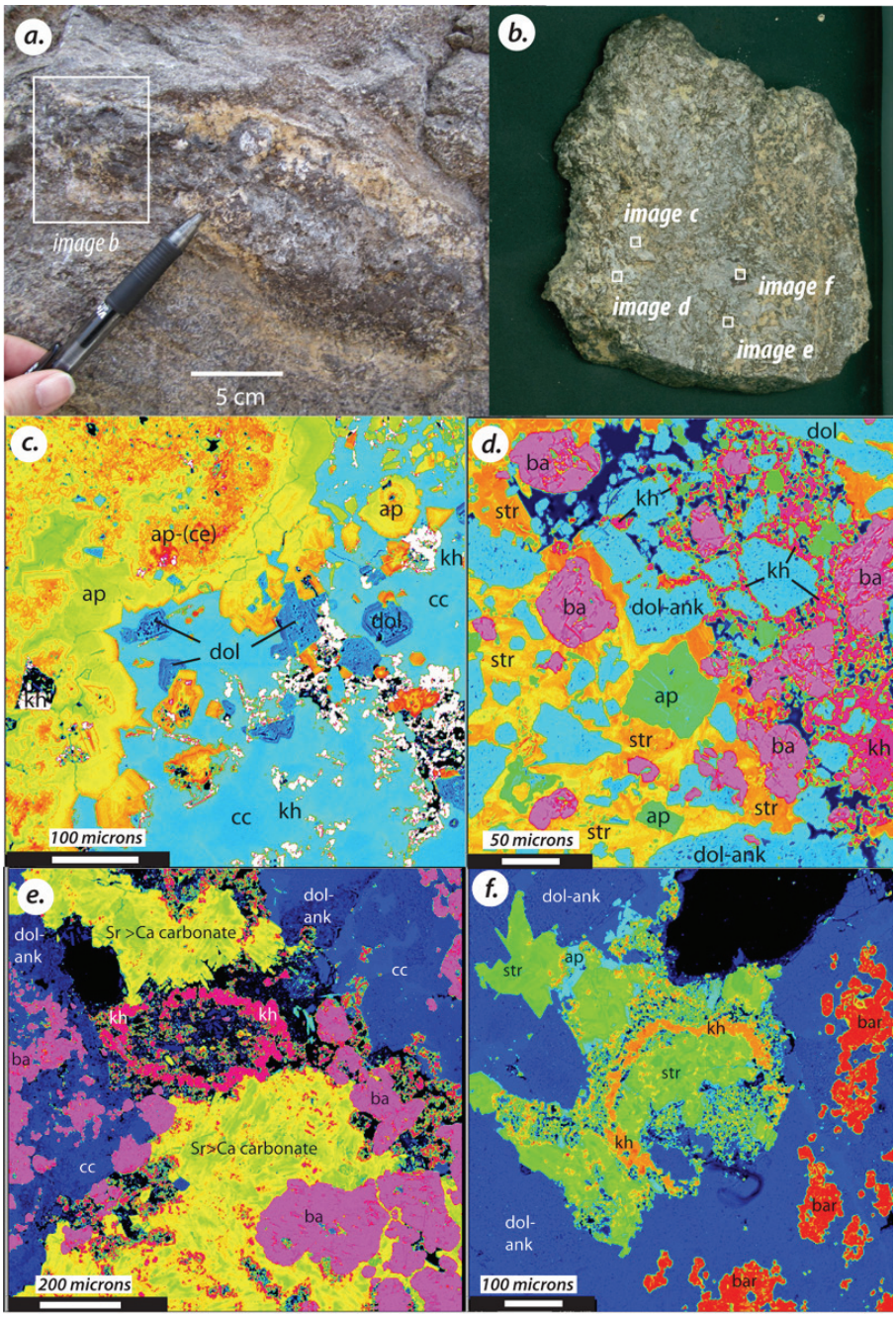

Figure 21A–6. Mineralogy and crystallization sequence of the concordantly REE-mineralized rock, RT-11K-2, February 2011 traverse. (*a*) Photograph of the concordant symmetric bands of mineralized alvikite. (*b*) Slab of the symmetrically zoned band, outlined in 6*a*, showing the (approximate) location of the false-colored backscattered electron images (*c*-*f*). (*c*) False-colored backscattered electron image of box *c*, dark band of apatite, dolomite, and calcite: apatite (ap), apatite-(Ce) (ap-(Ce)), dolomite (dol), khanneshite (kh), and calcite (cc). Calcite and khanneshite appear as late, interstitial minerals after early-formed phenocrysts of dolomite and apatite. (*d*) False-colored backscattered electron image of box *d*: dolomitic ankerite (dol-ank), apatite (ap), barite (ba), strontianite (str) and, khanneshite (kh). Barite, strontianite, and khanneshite appear as an infilling of late minerals into brecciated dolomitic ankerite of the host alvikite. (*e*) False-colored backscattered electron image of box *e*, light-colored band: Sr-rich orthocarbonate (Sr >Ca carbonate), barite (ba), dolomitic-ankerite (dol-ank), calcite (cc), and khanneshite (kh). (*f*) False-colored backscattered electron image of box *f*, dark-colored band: barite (ba), dolomitic-ankerite (dol-ank), apatite (ap), strontianite (str), and khanneshite (kh). The dark bands consist mostly of dolomitic ankerite and barite, with interstitial strontianite, apatite, and immiscible droplets of khanneshite and strontianite. Photographs by Robert D. Tucker, U.S. Geological Survey.

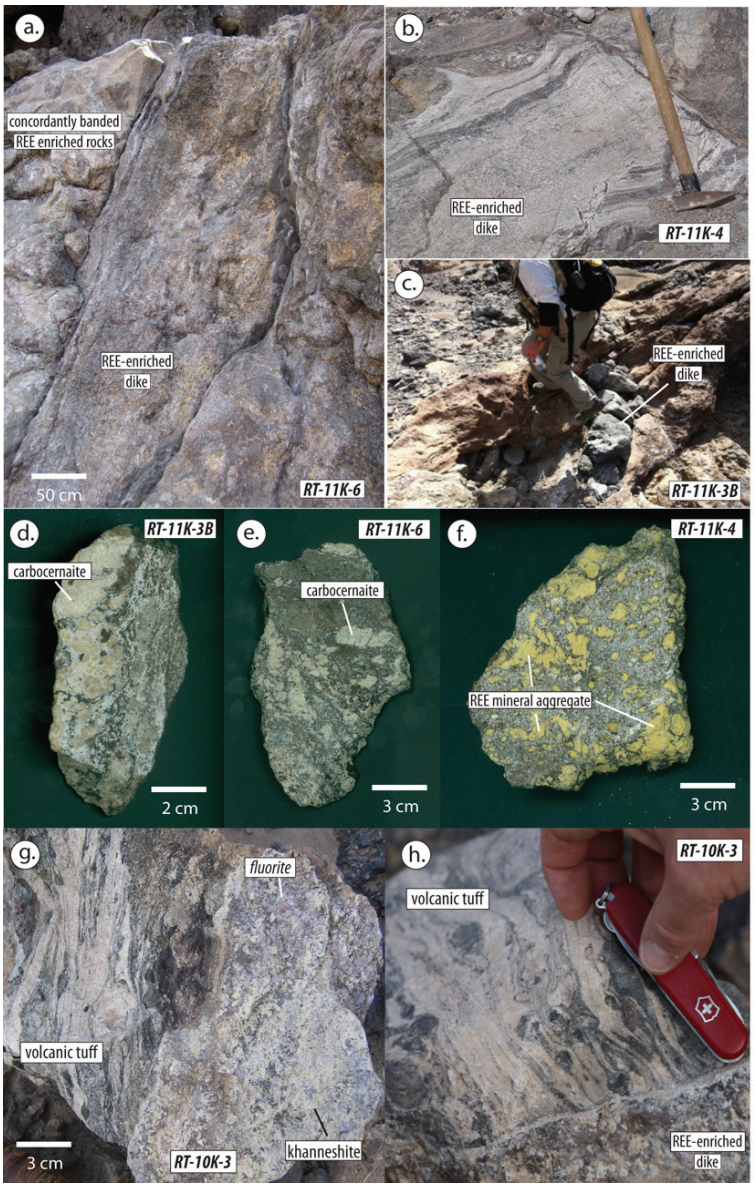

Figure 21A–7. Examples of discordant REE mineralization (Type 2) in the marginal zone of the central intrusive vent, February 2011 traverse, (fig. 21A-2). (*a*) The apatite-rich discordant carbonatite dike, with local pegmatitic texture, at outcrop RT-11K-6. The carbonatite dike, approximately 75 centimeters thick and steeply dipping, has relic igneous texture and demonstrable intrusive contacts with the concordantly banded alvikite (to the left). (*b*) An example of a fluorine-rich carbonatite dike, Khanneshin igneous complex (RT-11K-4), showing its intrusive nature into the banded alvikites of the marginal zone, central intrusive vent. (*c*) A thin apatite-rich dike (under the foot of the hiker) intruding yellow-weathering REE-enriched alvikite of the marginal zone, central intrusive vent (RT-11K-3B). (*d*) Slab of the apatite-rich carbonatite dike at RT-11K-3B showing the large phenocrysts of carbocernaite in a matrix of dolomitic-ankerite, apatite, barite, and strontianite. (*e*) Slab of the apatite-rich carbonatite dike at RT-11K-6 showing the large phenocrysts of carbocernaite in a matrix of dolomitic-ankerite, apatite, barite, and strontianite. (*f*) Slab of the fluorine-rich carbonatite dike at RT-11K-4 showing the large yellow-weathering phenocrysts of REE-carbonate in a fine-grained matrix of dolomite, barite, strontianite, and calcite. Also present, but too small to see at this scale, are phenocrysts of a former fluorine-bearing mineral now pseudomorphed by a strontium-rich orthocarbonate and an unidentified compound with potassium, magnesium, and fluorine. (*g*) Hand specimen of a fluorite- and khanneshite-bearing carbonatite dike (RT-10K-3) that has intruded discordantly across the volcanic layering of the layered volcanic tuffs (alvikite). (*h*) Close-up of the fluorine-rich dike and its contact with the layered volcanic tuff. Photographs by Robert D. Tucker, U.S. Geological Survey.

A magmatic origin is clearly indicated for Type 2 discordant dikes and tabular sheets (fig. 21A–8). Based on textural and field evidence, we suggest that the semiconcordant veins and discontinuous seams (Type 1 mineralization) may have formed in the presence of REE-rich hydrothermal fluids. It is possible that both types of REE mineralization may be penecontemporaneous, having formed in the marginal zone of a carbonate-rich magma, highly charged with volatile constituents (for example, carbon dioxide and fluorine), and strongly enriched in barium, strontium, and the LREE (La, Ce, Pr, and Nd).

21A.5.4.2 Grade of Barium, Strontium, and REE Enrichment

The grades in both types of REE-mineralized rocks are extraordinarily high and comparable to the world-class ores from Mountain Pass, California (USA) and Bayan Obo (China) (figs. 21A–9, 21A–10). Like both of these REE deposits, the barite-alvikites at Khanneshin are highly enriched in the light rare earth elements (LREE), over heavy rare earth elements (HREE). In contrast, the alvikites of the northeast part of the central vent are also highly enriched in barium and strontium (table 21A–1).

Type 1 mineralized rocks average 19.92 weight percent Ba, 3.61 weight percent Sr, and 2.78 weight percent ∑ LREE (the sum of La, Ce, Pr, and Nd). The average values of ∑ LREE for eight of our samples range between 6.22 and 1.83 weight percent (table 21A–2).

Type 2 mineralized rocks average 11.1 weight percent Ba, 5.46 weight percent Sr, and 3.28 weight percent ∑ LREE (the sum of La, Ce, Pr, and Nd). The average values of ∑ LREE for 14 of our samples range between 5.98 and 0.49 weight percent (table 21A–2).

Table 21A–1. Minerals containing rare earth elements, strontium, or barium as major elements at the Khanneshin complex.

Mineral	Formula	Theoretical REE_2O_3 (weight percent)
carbocernaite	$(Ca,Na)(Sr,Ce,Ba)(CO_3)_2$	18.64
ancylite-(Ce)	$Sr(Ce)\ (CO_3)_2\ (OH) \cdot H_2O$	47.98
calkinsite-(Ce)	$(Ce,La)_2\ (CO_3)_3\ .\ 4H_2O$	61.62
synchysite-(Ce)	$Ca(Ce,La)(CO_3)_2F$	52.64
parisite-(Ce)	$Ca(Ce,La)_2(CO_3)_3F_2$	60.89
bastnäsite-(Ce)	$(Ce, La)\ CO_3\ F$	74.81
apatite-(Ce)	$(Ca,Ce)_5PO_3F$	< 5
strontianite	$SrCO_3$	
barite	$BaSO_4$	
celestine	$SrSO_4$	

[1]Belovitskaya and others, 2002; [2] Yeremenko and Bel'ko, 1983; [3] Mandarino, 1995.

21A.5.4.3 Preliminary Resource Estimation

Tucker and others (2011) calculated a new estimation of the REE resource at Khanneshin based on field and analytical work conducted from 2009 to 2011. Because rocks in the Khanneshin Carbonatite Area of Interest have not been mapped in detail, drilled for exploration, or investigated using modern geophysical methods, the estimation is necessarily preliminary with various inferred assumptions. The calculation to convert rock volume to LREE resource involves converting volume to mass, via a density conversion factor, and then mass to a theoretical quantity of recoverable resource using an average grade of total LREE content (tables 21A–2 and 21A–3).

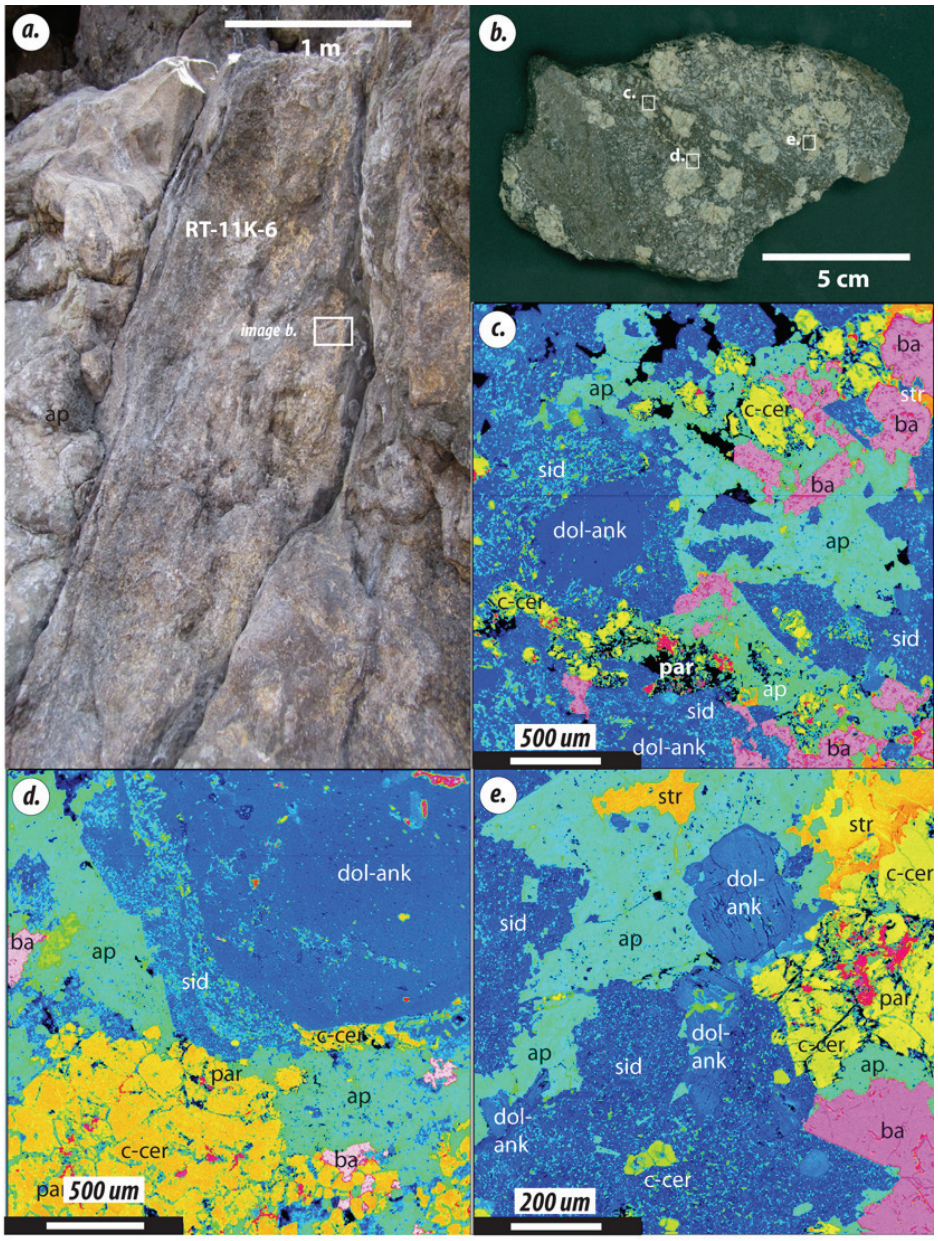

Figure 21A–8. Mineralogy and crystallization sequence of the apatite-rich intrusive dikes, Khanneshin complex. (*a*) Outcrop of intrusive dike RT-11K-6. The rectangle of image *b* shows the approximate location of the hand specimen pictured in *b*. (*b*) Rock slab of sample RT-11K-6 showing the phenocrysts of carbocernaite-(Ce) in a matrix of dolomitic-ankerite, siderite, apatite, and barite. Location of images *c*, *d*, and *e* are shown as the inset boxes. (*c*) False-colored backscattered electron image showing the textural relationships among carbocernaite-(Ce) (c-cer), dolomite-ankerite (dol-ank), apatite (ap), siderite (sid), barite (ba), and parisite-(Ce) (par). Dolomitic ankerite, with siderite rims, and carbocernaite-(Ce) are early phenocrysts; apatite and barite are interstitial minerals; and parasite-(Ce) is a late-stage alteration mineral of carbocernaite-(Ce). (*d*) False-colored backscattered electron image showing the textural relationships among carbocernaite-(Ce) (c-cer), dolomite-ankerite (dol-ank), siderite (sid), barite (ba), and apatite (ap). Dolomitic ankerite, with siderite rims, and carbocernaite-(Ce) are early phenocrysts; apatite, and barite are interstitial minerals; and parasite-(Ce) is a late- stage alteration mineral of carbocernaite-(Ce). (*e*) False-colored backscattered electron image showing the textural relationships among carbocernaite-(Ce) (c-cer), dolomite-ankerite (dol-ank), siderite (sid), barite (ba), strontianite (str), apatite (ap), and parasite-(Ce) (par). Dolomitic ankerite, with siderite rims, and carbocernaite-(Ce) are early phenocrysts; apatite, barite, and strontianite form interstitial minerals; parasite-(Ce) is a late-stage alteration mineral of carbocernaite-(Ce). Photographs by Robert D. Tucker, U.S. Geological Survey.

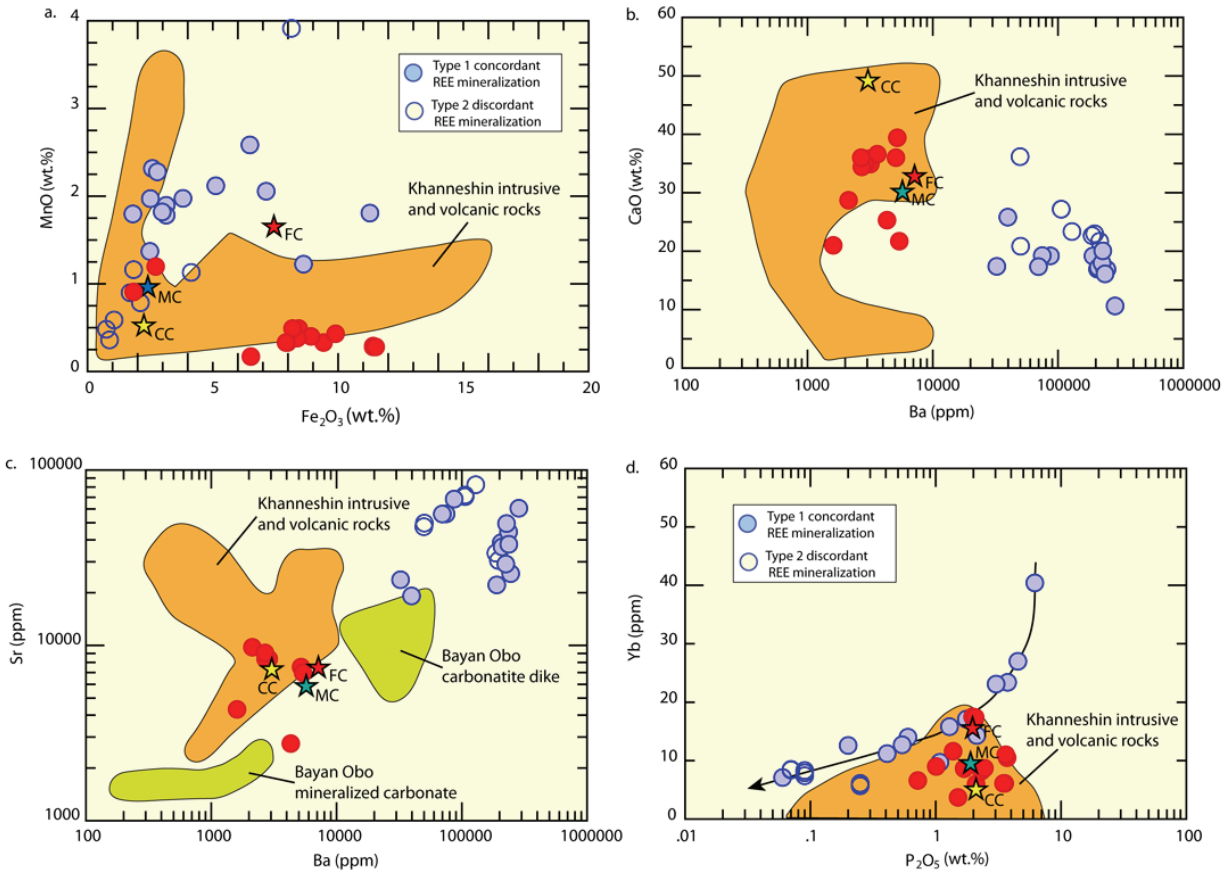

Figure 21A–9. Variations in major- and trace-element concentrations between normal alvikite and sövite of the Khanneshin carbonatite and the light rare earth element (LREE)-enriched rocks of the marginal central vent. Red circles are volcanic tuffs and dikes from the southwest part of the complex (Traverse 1, September 2009). Blue circles, filled and unfilled, are LREE-enriched rocks from the LREE zone. The shaded orange area is the field for Khanneshin intrusive and volcanic rocks sampled in 2009 and 2010. Also shown is average calcio-carbonatite (CC, yellow star), ferro-carbonatite (FC, red star), and magnesio-carbonatite (MC, blue star) from Woolley and Kempe (1989). (*a*) MnO (weight percent) versus Fe_2O_3 (weight percent). Note the strong enrichment in MnO of the REE-enriched rocks over the common alvikites of the Khanneshin carbonatite complex. (*b*) CaO (weight percent) versus barium (parts per million). Note the very high concentrations of barium, relative to CaO, in the REE-enriched rocks of the Khanneshin carbonatite. One percent (parts per hundred) equals 10,000 ppm (parts per million). Symbols same as figure 21A-9*a*. (*c*) Strontium (parts per million) versus barium (parts per million). Note the very high concentrations of barium, relative to strontium, in the REE-enriched rocks of the Khanneshin carbonatite. Also shown are concentrations in carbonatite dike at Bayan Obo (China) (data from Yang and others, 2009). One percent (parts per hundred) equals 10,000 ppm. Symbols same as figure 21A-9*a*. (*d*) Ytterbium (parts per million) versus log P_2O_5 (weight percent). Note the strong correlation between ytterbium and P_2O_5 in the REE-enriched rocks of the Khanneshin carbonatite, suggesting control by apatite. The concordantly banded rocks, and those intrusive dikes having modal apatite and carbocernaite, are enriched in ytterbium, a proxy for the HREE. The fluorine-rich intrusive dikes, bearing either fluorite or the unnamed potassium, magnesium, fluorine phase, are poor in apatite (lower P_2O_5 values) and hence they have lower HREE concentrations. Symbols same as figure 21A-9*a*.

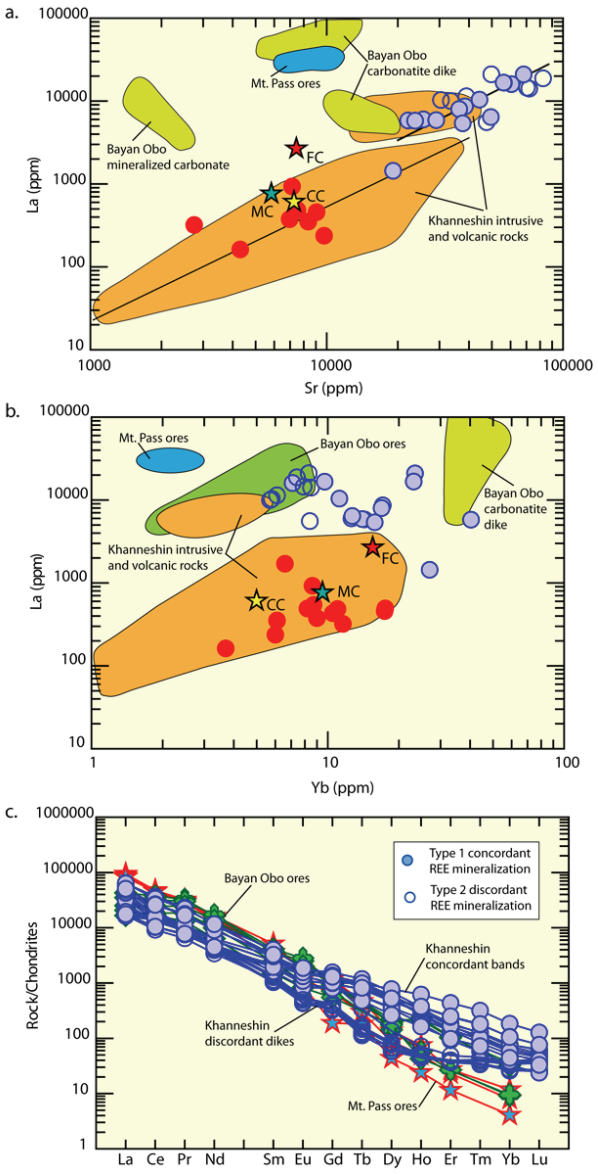

Figure 21A–10. Diagrams illustrating the magnitude and significance of REE enrichment in the marginal zone, central intrusive vent, Khanneshin complex. Red circles are volcanic tuffs and dikes from the southwest part of the complex (Traverse 1, September 2009). Blue circles, filled and unfilled, are LREE-enriched rocks from the LREE zone. The shaded orange area is the field for Khanneshin intrusive and volcanic rocks sampled in 2009 and 2010 (Traverses 2 and 3). Also shown is average calcio-carbonatite (CC, yellow star), ferro-carbonatite (FC, red star), and magnesio-carbonatite (MC, blue star) from Woolley and Kempe (1989). (*a*) Lanthanum (parts per million) versus strontium (parts per million). The positive correlation of the LREE and strontium in the REE-enriched rocks indicates the propensity of the LREE to substitute for strontium in khanneshite (burbankite group) and carbocernaite, the primary carbonate minerals, of the Khanneshin complex. Also shown are mineralized carbonate and carbonatite dikes from Byan Obo (data from Yang and others, 2009) and average ores from Mountain Pass, California (data from Castor, 2008). (*b*) Lanthanum (parts per million), representative of the LREE, versus ytterbium (parts per million), representative of the HREE. Common alvikites of the Khanneshin complex have LREE and HREE concentrations similar to average ferro-, magnesio-, and calcio-carbonatites worldwide. However, the ankerite-barite alvikites of the marginal central vent, Khanneshin complex, are highly enriched in the REE and comparable in grade to the world-class REE deposits of Bayan Obo (data for average Bayan Obo ores from Yuan and others, 1992) and Mountain Pass (data from Castor, 2008). (*c*) The Khanneshin whole-rock concentrations, February 2011 traverse, normalized relative to chondrite values. Same symbols as *b*, above. Also shown are the minimum, mean, and maximum grades of the REE ores from Mountain Pass and Bayan Obo (data sources as in *b*).

Table 21A–2. Barium, strontium, and rare earth element (REE) concentrations in whole rocks from the zone of light rare earth element (LREE) enrichment from the February 2011 scoping mission at the Khanneshin carbonatite area of interest.
[ppm, parts per million; wt. %, weight percent]

	Occurrence type	Ba wt.%	Sr wt.%	La ppm	Ce ppm	Pr ppm	Nd ppm	Sm ppm	Eu ppm	Gd ppm	Tb ppm	Dy ppm	Ho ppm	Er ppm	Tm ppm	Yb ppm	Lu ppm	La wt. %	Ce wt. %	Pr wt. %	Nd wt. %	∑ LREE wt. %
RT-11K-1A1	2	19.62	3.05	10,300	14,600	1,110	2,880	258	40109		6.9	26.4	3.4	8.3	1.01	5.8	0.86	1.030	1.460	0.111	0.288	2.889
RT-11K-1A2	2	21.51	3.90	11,400	15,800	1,190	3,040	267	42115		7.5	28.4	3.6	8.5	1.06	6.1	0.91	1.140	1.580	0.119	0.304	3.143
RT-11K-1B2	2	18.74	3.36	10,000	14,700	1,160	3,050	278	43109		7.7	28.7	3.5	8.4	1.02	5.7	0.88	1.000	1.470	0.116	0.305	2.891
RT-11K-2A2	1	19.04	2.21	5,820	8,880	840	2,740	390	75223		27.4	124	15.8	30.5	3.03	14.3	1.64	0.580	0.888	0.084	0.274	1.826
RT-11K-2B1	1	20.70	3.85	8,620	11,700	1,010	3,090	415	85271		36.5	162	20.8	40.4	3.84	17.1	2.06	0.860	1.170	0.101	0.309	2.440
RT-11K-2B2	1	21.01	3.64	7,980	11,200	992	3,060	417	85267		36.2	160	20.9	39.8	3.83	16.9	2.11	0.790	1.120	0.099	0.306	2.315
RT-11K-3B31	2	23.63	4.43	10,400	12,200	945	2,710	445	107367		47.5	181	18.6	30.9	2.47	11.2	1.36	1.040	1.220	0.095	0.271	2.626
RT-11K-3B32	2	28.57	6.05	16,000	16,600	1,180	3,040	328	65221		27	118	13.0	20.7	1.72	7.1	0.81	1.600	1.660	0.118	0.304	3.682
RT-11K-4AO1	2	4.99	4.75	5,550	7,940	720	2,160	231	3891.7		6.1	22.8	3.1	8.6	1.24	8.4	1.34	0.550	0.794	0.072	0.216	1.632
RT-11K-4AO2	2	12.92	8.24	18,800	17,600	1,170	2,770	217	34108		6.1	23.1	3.3	8.3	1.16	7.4	1.21	1.880	1.760	0.117	0.277	4.034
RT-11K-4B3	2	10.63	7.05	14,500	14,500	1,020	2,540	216	3495.8		5.7	23.1	3.4	9.0	1.23	7.9	1.30	1.450	1.450	0.102	0.254	3.256
RT-11K-4C1A	2	10.61	7.20	14,100	13,900	995	2,470	210	3390.1		5.3	20.2	3.1	8.4	1.25	8.5	1.43	1.410	1.390	0.100	0.247	3.147
RT-11K-4C1B	2	3.98	1.91	1,440	2,360	244	838	189	49166		24.4	120	18.6	44.3	5.23	27	3.53	0.144	0.236	0.024	0.084	0.488
RT-11K-5A2	1	24.59	2.57	5,990	13,000	1,240	3,690	507	110349		44.1	181	19.9	32.8	2.83	12.6	1.57	0.599	1.300	0.124	0.369	2.392
RT-11K-5A3	1	22.44	2.91	5,870	12,400	1,190	3,580	512	112369		47.8	201	22.3	36.7	3.29	14	1.67	0.587	1.240	0.119	0.358	2.304
RT-11K-5B1B	1	23.73	3.77	5,380	11,900	1,180	3,600	508	109352		46.2	201	23.8	42.3	3.7	15.8	1.80	0.538	1.190	0.118	0.360	2.206
RT-11K-5B3B	1	22.79	4.95	6,400	13,300	1,270	3,990	626	136431		55.5	236	25.5	38.2	3.01	12.7	1.52	0.640	1.330	0.127	0.399	2.496
RT-11K-5B6A	1	5.03	4.98	21,000	31,500	2,600	7,090	657	102274		15.8	46.5	5.0	11.0	1.36	8.3	1.36	2.100	3.150	0.260	0.709	6.219
RT-11K-6A2A	2	3.25	2.37	5,790	9,030	870	2,810	397	84279		46.4	266	43.3	98.1	9.48	40.4	4.33	0.579	0.903	0.087	0.281	1.850
RT-11K-6A2B	2	8.70	6.82	20,900	29,100	2,480	7,300	816	140376		37.5	175	25.7	54.6	5.32	23.4	2.59	2.090	2.910	0.248	0.730	5.978
RT-11K-6B2	2	7.49	5.62	16,600	23,000	1,980	5,800	615	102279		22.5	90.8	11.4	22.0	2.16	9.7	1.12	1.660	2.300	0.198	0.580	4.738
RT-11K-6B3	2	7.00	5.61	16,700	22,400	1,890	5,680	660	120358		38.5	180	26.2	56.0	5.43	23.1	2.60	1.670	2.240	0.189	0.568	4.667

	Δ Ba wt.%	Δ Sr wt.%		Δ La wt.%	Δ Ce wt.%	Δ Pr wt.%	Δ Nd wt.%	Δ LREE
	15.50	4.51	Total collection	1.091	1.491	0.125	0.357	3.063
	19.92	3.61	Type 1 mineralized rocks (# 2,5)	0.837	1.424	0.129	0.386	2.775
	11.07	5.46	Type 2 mineralized dikes (# 3,4,6)	1.279	1.533	0.123	0.347	3.282
	19.96	3.44	Fluorine-rich dikes (#1)	1.057	1.503	0.115	0.299	2.974

Table 25A–3. Estimated LREE resources of the Khanneshin complex.

[g/t, grams per cubic centimeter; km, kilometers; m^3, cubic meters; Mt, million metric tons; wt. %, weight percent]

	Length (km)	Width (km)	Depth (km)	Volume (m^3)	Density, (g/cm^3)	Rock quantity Mt	Δ LREE grade† (wt.%)	Mt LREE (before 10:1 dilution)#	Mt LREE (after 10:1 dilution)
LREE enriched box									
Type 1. Concordant veins and seams:									
	0.750	0.550	0.150	0.061875	2.94	181.913	2.775	5.048	0.505
	0.330	0.250	0.150	0.012375	2.94	36.383	2.775	1.010	0.101
Total LREE box				0.074250	2.94	218.295	2.775	6.058	0.606
Type 2. Discordant veins and seams*									
#1	0.050	0.020	0.150	0.000150	2.94	0.441	3.282		0.014
#2	0.500	0.040	0.150	0.003000	2.94	8.820	3.282		0.289
#3	0.400	0.035	0.150	0.002100	2.94	6.174	3.282		0.203
Total discordant sheets				0.005250	2.94	15.435	3.282		0.507
Total LREE box$									1.113$
Remote sensing polygons									
Northwest of the Soviet-defined box				0.071176	2.94	209.257	2.775	5.807	0.581
Within the Soviet-defined box				0.073124	2.94	214.985	2.775	5.966	0.597
Total remote sensing polygon									1.178

†Taken from table 21A–2.

#Wall rock is 10 times more abundant than mineralized seams, hence 10:1 dilution factor

*Estimated from mineral content in dikes, not affected by wall rock dilution

$Sum of Type 1 and Type 2 tonnage

Soviet geologists delineated an area (fig. 21A–2), approximately 0.64 km^2, within which ankerite-barite carbonatite is macroscopically enriched in REE-bearing carbonate minerals. Within this area the total LREE concentrations in many rocks approach several percent, with barium and strontium concentrations averaging 15.5 and 4.51 weight percent, respectively (table 21A–2).

21A.5.4.3.1 Concordant Layers of Mineralization

Concordant mineralization consists of yellow-weathering REE-carbonates (± fluorine) that form layer-parallel, centimeter-thick bands, which alternate with dark, meter-thick layers of ankerite-barite alvikite (wall rock). Based on USGS field observations and the Soviet work, whose field teams accurately described the geology and mineralogy of the entire igneous complex, we assert this style of mineralization is common throughout the area of REE enrichment. This assumption is borne out by the many samples of "REE ore" recovered and analyzed by Soviet geologists in the area and by our own collection that confirms their data. The volume of REE mineralization, however, must be diluted by a factor of 10, which is approximately the ratio of concordantly mineralized rock to weakly mineralized wall rock (fig. 21A–5*d*). This dilution factor is a conservative value because, in some sections, concordant mineralization is ubiquitous, whereas, in other sections, surface exposures are poor or covered by alluvium. The proper way to determine directly this dilution factor is to drill and assay recovered rock core throughout the area. It was not possible to do this for our study because of budgetary, logistical, time, and security concerns.

Because drilling, core analysis, and geophysical exploration were not possible, the depth of mineralization throughout the REE zone is estimated from ground observations. We assert a value of 150 m based on the vertical dimension of mineralized rock observed over the rugged relief of the region (approximately 170 m). In essence, we assume a depth of mineralization that roughly mimics the surface topography of the area of REE enrichment. This assumption is justified because the topography is young (less than 5 million years), the valley walls are steep, and hence the mass of eroded rock is small relative to the unexhumed mass at depth. We believe, moreover, our estimate is conservative if, as seems

likely, the zone of REE enrichment extends to depths well beyond the arbitrary value of the local relief (fig. 21A–3). The proper means to determine the depth of mineralization is to drill and assay core throughout the region of REE enrichment.

Using an average density of mineralized carbonatite (2.94 grams per cubic centimeter, g/cm^3), an average grade of LREE concentration (2.775 weight percent, table 21A–2), and a dilution factor of 10:1 (wall rock: mineral bands), we calculate approximately 0.505 Mt (million metric tons) of LREE are present in the concordantly mineralized rocks of the Soviet-defined zone (table 21A–3).

21A.5.4.3.2 Discordant Tabular Sheets

Within the zone of REE enrichment, Soviet geologists identified more than 50 "ore bodies" of a stockwork-type with widths between 60 and 0.5 m and lengths between 500 and 20 m. The vertical dimension of the stockwork bodies is not given, but they are likely to be hundreds of meters deep, as they form near-vertical dikes (fig. 21A–7) across the rugged relief of the region. These bodies correspond to the discordant, steeply dipping tabular sheets of this report, which are decimeters to meters thick and meters to hundreds of meters long.

Three major stockwork bodies of this type were trenched and sampled by the Soviet teams (Cheremitsyn and Yeremenko, 1976):

Stockwork dike # 1, located in the northwest part of the REE zone, is 20 m by 50 m with a northwest strike and near-vertical dip. Ten small trenches, each 2 m long, were dug across the dike. The LREE concentration (La plus Ce) for all of the Soviet samples averages more than 1.5 weight percent (Cheremitsyn and Yeremenko, 1976).

Stockwork dike #2, located in the northern part of the REE zone, is 10-60 m wide and 500 m long; it has a north-south strike and near-vertical dip. Three trenches were dug across the dike, in its northern, central, and southern part. The average concentration for La plus Ce for all of the trench samples is 1.5 weight percent (Cheremitsyn and Yeremenko, 1976).

Stockwork dike # 3, located in the southeast part of the REE zone, is ~35 m wide and 400 m long; it has a northeast strike and near-vertical dip. One trench across its central part yielded an average concentration for La and Ce of greater than 1.5 weight percent (Cheremitsyn and Yeremenko, 1976).

The Soviet analyses of the stockwork dikes yield LREE concentrations that are compatible with the average ∑LREE concentrations of the discordant dikes in our collection (3.282 average weight percent ∑LREE, table 21A–2).

Our estimate of LREE resources within the discordant tabular dikes (table 21A–3) is a conservative estimate because the calculation is only for the three largest dikes, and more than 50 such bodies are recognized. As with the resource calculation for the concordantly mineralized rocks, we assume the discordant dikes extend to 150 m depth and that LREE concentrations are uniform throughout the mass of rock.

Assuming an average density for carbonatite (2.94 g/cm^3) and an average grade of ∑LREE concentration (3.282 weight percent, table 21A–2), we estimate approximately 0.507 Mt of LREE are present in the three largest dikes (discordant sheets) of the Soviet-defined zone (table 21A–3).

Thus, together with the concordantly mineralized rocks, we estimate a LREE resource of 1.1 Mt in the entire Soviet-defined REE zone. This estimate comports well with the probabilistic estimate of 1.4 Mt of undiscovered REE resources in all of south Afghanistan (Peters and others, 2007). In addition to the LREE, the Khanneshin carbonatite is greatly enriched in barium (> 10 weight percent), strontium (> 6 weight percent), phosphorus (~ 2 weight percent), and uranium (> 0.05 weight percent). A resource calculation of these elements was not attempted.

21A.6 Summary of Potential

The presence of relatively well-explored REE and uranium prospects at the Khanneshin Carbonatite Area of Interest and its subareas is an important positive indicator for this area. The

petrologic characteristics of the associated igneous rocks and the available assays suggest that a REE deposit of significant size may be present.

The USGS assessment team (Peters and others, 2007) estimated that there is a 90-percent chance of 0 or more undiscovered porphyry copper deposits at Khanneshin, a 50-percent chance of 1 or more, and a 10-percent chance of two or more deposits. The amounts of contained metal that result from a Monte Carlo simulation based on this estimate are illustrated and summarized in table 21A–4. This is a relatively optimistic estimate for a relatively small area.

Table 21A–4a. The statistical parameters for the assessment of the Khanneshin permissive tract.
[Data are from Peters and others (2007)]

Probability (percent)	Estimated number of deposits
90	0
50	1
10	2
5	3
1	5

Table 21A–4b. Estimated mean metric tons of undiscovered mineralized rock, phosphate, rare earth elements (REE), and niobium in undiscovered deposits of the Khanneshin complex.
[Data are from Peters and others (2007). Values are rounded to no more than three significant digits. Nb, niobum; P, phosphorus]

Rock (metric tons)	P (metric tons)	REE (metric tons)	Nb (metric tons)
251,000,000	6,200,000	1,400,000	3,500,000

These estimates were used to generate probabilistic estimates of the amounts of phosphorus, REE, and niobium in the undiscovered deposits using Monte Carlo simulation (table 21A–4*b*).

Based on several assumptions, and employing a simple geometry for volume of mineralized rock, the present report estimates at least 1 Mt (million metric tons) of LREE are present in the Khanneshin Carbonatite Area of Interest (Tucker and others, 2011).

Future discoveries and delineations of resources with the Khanneshin Carbonatite Area of Interest require aeromagnetic and aeroradiometric surveys flown at low elevation, coupled with detailed geologic mapping,, explatory drilling, and ground geochemical surveys.

21A.7 References Cited

Abdullah, J., Bordet, P., Carbonnel, J.P., and Pias, J., 1975, Sur l'existence d'un dôme recent de carbonatites dans le Registan (Afghanistan du Sud) [The existence of a Recent carbonatite dome in Registan (southern Afghanistan): Sciences Naturelles, v. 281, no. 23, p. 1801–1804.

Abdullah, Sh., Chmyriov, V.M., Stazhilo-Alekseev, K.F., Dronov, V.I., Gannan, P.J., Rossovskiy, L.N., Kafarskiy, A.Kh., and Malyarov, E.P., 1977, Mineral resources of Afghanistan (2d ed.): Kabul, Afghanistan, Republic of Afghanistan Geological and Mineral Survey, 419 p.

Alkhazov, V. Yu, Atakishiyev, Z.M., and Azimi, N.A., 1978, Geology and mineral resources of the early Quaternary Khanneshin carbonatite volcano (southern Afghanistan): International Geology Review, v. 20, no. 3, p. 281–285.

Belovitskaya, Yu.V., Pekov, I.V., Gobechiya, E. R., Kabalov, Yu.K., Schneider, J., 2002, Determination of the crystal structure of Khanneshite by the Rietveld method: Crystallography Reports, v. 47, no. 1, p. 39–42. [Translated from Kristallografiya, 2002, v. 47, no. 1, p. 46–49.]

Castor, S.B., 2008, The Mountain Pass rare-earth carbonatite and associated ultrapotassic rocks California: The Canadian Mineralogist, v. 46, p. 779–806.

Cheremitsyn, V.G., and Yeremenko, G.K., 1976, Report of the Hanneshin crew on the results of prospecting and evaluational activity for 1976 [in Russian]: Kabul, Afghanistan, Afghanistan Geological Survey Report 1142, 84 p. and 7 maps, scale 1:10,000.

Chmyrev, V.M., 1976, Report of the Nuristan crew on the results of geological prospecting for solid commercial mineral deposits in Afghanistan, 1975 [in Russian]: Kabul, Afghanistan, Afghanistan Geological Survey Report 1028, Section B, no. 5, p. 92–103.

Dunn, P.J., Fleischer, M., Chao, G.Y., Cabri, L.J., and Mandarino, J.A., 1983, New mineral names: American Mineralogist, v. 68, p. 1248–1252.

Hogarth, D.D., 1986, Mineralogy of carbonatites—A review: Geological Association of Canada, Mineralogical Association of Canada, and Canadian Geophysical Union Joint Annual Meeting Program and Abstracts, v. 11, p. 82.

Mandarino, J A., 1995, New minerals recently approved by the Commission on New Minerals and Mineral Names, International Mineralogical Association: The Canadian Mineralogist, v. 33, pt. 1, p. 189–192.

Peters, S.G., Ludington, S.D., Orris, G.J., Sutphin, D.M., Bliss, J.D., and Rytuba, J.J., eds., and the U.S. Geological Survey-Afghanistan Ministry of Mines Joint Mineral Resource Assessment Team, 2007, Preliminary non-fuel mineral resource assessment of Afghanistan: U.S. Geological Survey Open-File Report 2007–1214, 810 p., 1 CD–ROM. (Also available at *http://pubs.usgs.gov/of/2007/1214/*.)

Singer, D.A., 1986a, Descriptive model of carbonatite deposits, *in* Cox, D.P., and Singer, D.A., eds., Mineral deposit models: U.S. Geological Survey Bulletin 1693, p. 51.

Singer, D.A., 1986b, Grade and tonnage model of carbonatite deposits, *in* Cox, D.P., and Singer, D.A., eds., Mineral deposit models: U.S. Geological Survey Bulletin 1693, p. 52–53.

Sweeney, R.E., Kucks, R.P., Hill, P.L., and Finn, C.A., 2006, Aeromagnetic and gravity surveys in Afghanistan—A web site for distribution of data: U.S. Geological Survey Open-File Report 2006-1204, available at *http://pubs.usgs.gov/of/2006/1204/*.

Tucker, R.D., Belkin, H.E., Schulz, K.J., Peters, S.G., and Buttleman, K.P., 2011, Rare earth element mineralogy, geochemistry, and preliminary resource assessment of the Khanneshin carbonatite, Helmand Province, Afghanistan: U.S. Geological Survey Open-File Report 2011–1207, available at *http://pubs.usgs.gov/of/2011/1207/*.

Vikhter, B.Y., Yeremenko, G.K., and Chmyrev, V.M., 1976, A young volcanogenic carbonatite complex in Afghanistan: International Geology Review, v. 18, no. 11, p. 1305–1312.

Vikhter, B.Y., Yeremenko, G.K., Chmyrev, V.M., and Abdulla, D., 1978, Pliocene–Quaternary of Afghanistan: International Geology Review, v. 20, no. 5, p. 525–536.

Whitney, J.W., 2006, Geology, water, and wind in the lower Helmand Basin, southern Afghanistan: U.S. Geological Survey Scientific Investigations Report. 2006–5182, 40 p., available at *http://pubs.usgs.gov/sir/2006/5182/*.

Woolley, A.R., 1989, The spatial and temporal distribution of carbonatites, *in* Bell, Keith, ed., Carbonatites–Genesis and evolution: Unwin Hyman, London, p. 15–37.

Woolley, A.R., and Kempe, D.R.C., 1989, Carbonatites—Nomenclature, average chemical compositions, and element distributions, *in* Bell, Keith, ed., Carbonatites—Genesis and evolution: London, Unwin Hyman, p. 1–14.

Yang, X-Y., Sun, W-D., Zhang, Y-X., and Zheng, Y-F., 2009, Geochemical constraints on the genesis of the Bayan Obo Fe-Nb-REE deposit in Inner Mongolia, China: Geochemica et Cosmochemica Acta, v. 73, p. 1417–1435.

Yeremenko, G.K., 1975, Brief characteristics of the Khanneshin carbonatite paleovolcano (in Russian): Report 1322, Afghanistan Geological Survey, Kabul, Afghanistan, 14 p. with 1 colored map, scale 1:10,000.

Yeremenko, G.E., Bel'ko, V A., 1983, Khanneshite $(Na,Ca)_3$ $(Ba,Sr,RE,Ca)_3$ $(CO_3)_5$—A new mineral of the burbankite group: International Geology Review, v. 25, no. 6, p.735–738.

Yuan, Zhongxin, Bai, Ge, Wu, Chenyu, Zhang, Zhonguin, and Ye, Xianjiang, 1992, Geological features and genesis of the Bayan Obo REE ore deposit, Inner Mongolia, China: Applied Geochemistry, v. 7, p. 429-442.